Computers in Biology and Medicine 114 (2019) 103473

Contents lists available at ScienceDirect

Computers in Biology and Medicine

journal homepage: www.elsevier.com/locate/compbiomed

Force-feedback assisted and virtual fixtures based K-wire drilling simulation

Johannes Maier [a,b,1], Jerome Perret [c,1], Michaela Huber [d], Martina Simon [e], Stephanie Schmitt-Rüth [e], Thomas Wittenberg [f], Christoph Palm [a,b,*]

[a] Regensburg Medical Image Computing (ReMIC), Ostbayerische Technische Hochschule Regensburg (OTH Regensburg), Galgenbergstr. 32, 93053 Regensburg, Germany
[b] Regensburg Center of Biomedical Engineering (RCBE), OTH Regensburg and Regensburg University, Galgenbergstr. 32, 93053 Regensburg, Germany
[c] Haption GmbH, Dennewartstr. 25, 52068 Aachen, Germany
[d] Department of Trauma Surgery & Emergency Department, University Hospital Regensburg, Franz-Josef-Strauß-Allee 11, 93053 Regensburg, Germany
[e] Fraunhofer Center for Applied Research on Supply Chain Services SCS, Nordostpark 93, 90411 Nuremberg, Germany
[f] Fraunhofer Institute for Integrated Circuits IIS, Am Wolfsmantel 33, 91058 Erlangen, Germany

ARTICLE INFO

Keywords:
Medical training system
Virtual fixtures
Virtual reality
Force-feedback haptics
Minimally invasive hand surgery
K-wire drilling

ABSTRACT

One common method to fix fractures of the human hand after an accident is an osteosynthesis with Kirschner wires (K-wires) to stabilize the bone fragments. The insertion of K-wires is a delicate minimally invasive surgery, because surgeons operate almost without a sight. Since realistic training methods are time consuming, costly and insufficient, a virtual-reality (VR) based training system for the placement of K-wires was developed. As part of this, the current work deals with the real-time bone drilling simulation using a haptic force-feedback device.

To simulate the drilling, we introduce a virtual fixture based force-feedback drilling approach. By decomposition of the drilling task into individual phases, each phase can be handled individually to perfectly control the drilling procedure. We report about the related finite state machine (FSM), describe the haptic feedback of each state and explain, how to avoid jerking of the haptic force-feedback during state transition.

The usage of the virtual fixture approach results in a good haptic performance and a stable drilling behavior. This was confirmed by 26 expert surgeons, who evaluated the virtual drilling on the simulator and rated it as very realistic. To make the system even more convincing, we determined real drilling feed rates through experimental pig bone drilling and transferred them to our system. Due to a constant simulation thread we can guarantee a precise drilling motion.

Virtual fixtures based force-feedback calculation is able to simulate force-feedback assisted bone drilling with high quality and, thus, will have a great potential in developing medical applications.

1. Introduction

For every human being the unrestricted usability of its hand is essential in daily life. After an accident, bone fractures with displacement may result in mechanical impairments or limited flexibility of the hand. The most common way to treat these fractures and ensure recovery, surgeons are stabilizing broken bones with so-called Kirschner-wires (K-wires, Fig. 1a). In order to fix the fracture fragments (Fig. 1b) the K-wire is drilled into the bones using a two-dimensional X-ray image as visual guidance. For drilling, a K-wire is fixed within the drill chuck of a medical hand drill (Fig. 1c). During this delicate minimally invasive surgical intervention, the starting position and angle of the bone drilling are important in order not to harm risk structures such as tendons, nerves or vessels. Therefore, and due to the small sized bone structures in the hand, excellent manual skills are necessary [1–4].

Nowadays, innovative medical virtual reality (VR) simulators are available worldwide and are increasingly used to educate and train surgical interventions, e.g. laparoscopic or endoscopic interventions as well as dental drilling procedures [5–7]. The background for such training simulators are scientific studies observing users of video-games, who have a substantially superior eye-hand coordination than the control group. This eye-hand coordination is one crucial ability for surgeons [5,6,8–10].

* Corresponding author at: Regensburg Medical Image Computing (ReMIC), Ostbayerische Technische Hochschule Regensburg (OTH Regensburg), Galgenbergstr. 32, 93053 Regensburg, Germany.
E-mail address: christoph.palm@oth-regensburg.de (C. Palm).
[1] These authors contributed equally to the work.

https://doi.org/10.1016/j.compbiomed.2019.103473
Received 26 July 2019; Received in revised form 11 September 2019; Accepted 23 September 2019
Available online 25 September 2019

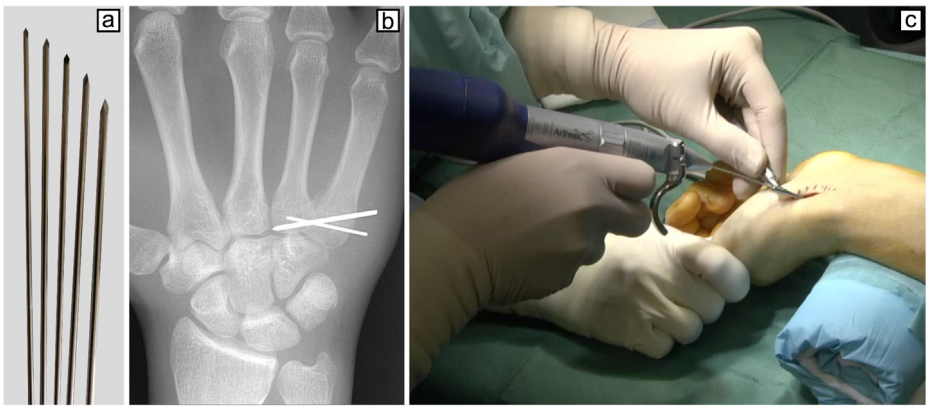

Fig. 1. Minimally invasive K-wire drilling. (a) K-wires with different diameter. (b) X-ray image of a patients hand after K-wire surgery. (c) Minimally invasive K-wire drilling in the operating room. The K-wire is located in the drill chuck of a medical hand drill and is brought close to the bone through a small stab incision. The rotation of the K-wire begins by pressing a continuously adjustable button on the hand piece. With a pin driver leverage the K-wire can be decoupled from the drill chuck to adapt the K-wire length.

Because there is currently no VR training simulator for the minimally invasive hand surgery available, we are developing a compact haptic and visual assisted training simulation system for complex bone drilling with K-wires for minimally invasive hand surgery (HaptiVisT) [3,11].

1.1. State of the art

VR-based drilling simulation in orthopedic training systems can be treated differently. *Tsai et al. (2007)* described a complete mathematical model to simulate the entire drilling process within an orthopedic training simulator [4]. His model makes it possible to accurately predict the forces and torques during bone drilling, as the load on the cutting lips and chisel edges are calculated. The resulting force components are transferred to a haptic output device. *Vankipuram et al. (2010)*, however, divided the complex drilling process into simple single subtasks to train only the basic drilling processes [12]. Training systems, which simulate the entire drilling process, are very effective and can give feedback on the complete drilling task, but they induce high costs through a large hardware setup. Furthermore, they are complex to simulate. Simulating individual subtasks simplifies the process and focuses only on basic skills to be learned. A completely different non-VR approach was developed by *Lopez et al. (2014)*, who tested a very low cost physical orthopedic training simulator [13]. With this, young surgeons can achieve senior skill level by training basic motor skills on a simulator purchased at a local hardware store.

Training simulators regarding to K-wire drilling as well as linear bone drilling and sawing were introduced by several authors. A force-feedback assisted K-wire drilling simulator for distal radius fractures was developed by *Seah et al. (2014)*. The force being applied to a haptic device is calculated using the distance between a haptic interaction point (position of the physical hand piece) and a virtual collision point [14]. *Wu et al. (2014)* introduced a virtual training system for maxillofacial surgery including bone cutting, drilling and milling under force-feedback calculation with regression equations [15]. *Lin et al. (2014)* considered in addition bone density, feed and rotation speed to compute haptic forces for bone sawing [16].

The work presented in this paper is part of the HaptiVisT project and deals with a real-time simulation of bone drilling and haptic force-feedback transmission to trainees by a haptic device. The most novel contributions of the paper are: (i) We decompose the complex bone drilling process with K-wires into a finite number of simple and logical subunits, which are located in a finite state machine (FSM). (ii) For the first time so-called *virtual fixtures* are used simulating an individual force-feedback of each subunit state. Our virtual fixtures approach guarantees a stable simulation of any complex task in real time, since they are easily prototyped or modified. (iii) This innovative virtual fixtures based force-feedback is tested and validated by an expert surgeon study. (iv) To simulate the drilling process absolutely realistic, we have determined real drilling feeds using a specially designed experimental setup and transferred them to the drilling simulation, comparing real and virtual drilling.

The paper is organized as follows: Section 2 presents theoretical details about the HaptiVisT system (Section 2.1), the decomposition of the drilling task into a FSM (Section 2.2), the virtual fixtures based haptic feedback (Section 2.3), the design of the expert surgeon study (Section 2.4) and the experimental pig bone drilling setup (Section 2.5). Sections 3 and 4 present a summarized video presentation of the virtual fixtures based K-wire drilling FSM and discuss the results of the corresponding expert study rating and of the experimental pig bone drilling. Finally, Section 5 states conclusions and future works.

2. Materials and methods

To transfer the basic K-wire drilling setup of the operating room to VR, the training system mock-up consists of several hardware components.

2.1. System mock-up

With a haptic force-feedback device, it is possible to transfer a three-dimensional (3D) position from the real world coordinate system into the computer's internal representation. Similarly, pre-calculated force components can be transferred from the computer to the haptic device, that the user can feel and touch virtual objects, which are only "real" in the visualization. Because of the necessity to render torques, we are using the haptic device "Virtuose 6D Desktop" by Haption© with force output on all six degrees-of-freedom (DOF) [17]. A 3D printed drilling machine replica of the Arthrex DrillSaw Mini 300™ is attached at the tip of the haptic device [18]. It transmits the rotation speed of the K-wire wirelessly to the computer and contains a vibration motor in order to generate a slight drilling vibration.

The drilling visualization is displayed on an autostereoscopic single-user 3D monitor [19]. This monitor is manufactured by the SeeFront GmbH and contains an eye tracking system used to steer a complex lenticular lens system [20]. Through that configuration the user does not require 3D glasses for depth perception. During a surgical intervention, surgeons need to feel important bony protrusions of the hand to find the best bore angle. Thus, and for real bimanual haptics, a 3D printed haptic hand phantom is arranged between user and the 3D screen [11].

A real-time optical tracking camera uses specially developed and positioned markers to transfer the hand position and rotation to the

computer system. This tracking approach enables positioning the visualized hand in such a way, that it follows the movement of the phantom. However, the drilling still takes place only in the visualization, since the associated K-wire is inserted only in the virtual drill chuck. In this way, K-wire drilling can be practiced repeatedly without destroying disposables or the hand phantom. For additional interaction between system and user, a graphical user interface (GUI) is provided on a touchscreen monitor, and can be used to create X-ray simulations and change drill bits or parameters of the system.

The real-time simulation of voxel erosion is based on the open source C++ framework chai3d [21] for computer haptics. Haptic and visual rendering are separated in independent threads to ensure a smooth simultaneous simulation. Driller, bones and skin of the hand are represented by a mixture of volume and surface rendering. For the essential collision detection between the bones and the driller we use the rigid body bullet physics engine (BPE) based on complex triangle meshes [22]. Further collision detection between the K-wire tip and a bone is realized by using massless haptic points from the chai3d library. The prototype setup, rendering and drilling process stages can be seen in Fig. 2. For further reading we refer to our recently published articles [3,23].

To identify the main task for K-wire drilling simulation, the real world procedure is analyzed in more detail.

2.2. Problem analysis and drilling decomposition

In real life, during hand surgery a K-wire is mounted on a drill handle and fixed within a drill chuck (Fig. 1c). The index finger is placed on a linear pushbutton, which regulates the rotation speed. The pin driver leverage, fixed at the drill head, can unlock the K-wire, to remove the K-wire or adjust its length. After placing the K-wire tip on the bone surface through a stab incision and adjusting the initial drill angle, the drilling process can be described as follows: Due to its very sharp tip and cutting edges, the K-wire does not slip aside and remains stuck on the bone surface. Only if the incident angle between the bone surface and the K-wire becomes too large the K-wire tip loses halt and slips over the bone surface and may injure the surrounding soft tissue. After activation of the drill rotation the K-wire immerges into the bone. If the penetration of the cortical bone is deep enough, the incidence angle can no longer be adjusted. Therefore, the K-wire can only be moved in axial forward or backward direction, if the rotation is active. Otherwise the K-wire is completely stuck inside the bone [24,25]. When removing the K-wire by pulling back the driller from the bore hole with activated drill rotation, friction between bone meal and K-wire can be felt.

We simulate this complex drilling process with the help of a finite state machine (FSM). In a FSM, sequences of any complexity can be subdivided into a finite number of simple logical states, which in sum are responsible for the system's behavior. The system can be in exactly one state and after starting its initial state, every other state can be reached across well-defined transitions. These state transitions are triggered by user actions [26–29].

For our K-wire drilling FSM in Fig. 3, six discrete states have been defined to describe the drilling process. These are "Free", "Point locked", "Axis locked", "Fully locked", "Shift wire" and "Align wire". The states can be explained as follows:

- "Free": Initially, the driller can be moved freely through the (real and virtual) 3D world. During this "Free" state, collisions between driller, the whole K-Wire and bones are simulated using the BPE [22]. The "Free" state remains active until a contact between tool tip and a bone occurs. The drill tip is superpositioned with an invisible haptic point of the framework chai3d [21]. Because of the volume bone models, the haptic point recognizes collisions with individual voxels [3]. As soon as the collision event is transmitted to the FSM, a state transition to "Point locked" is triggered.

Table 1
List of all Finite State Machine (FSM) transitions connecting the six discrete K-wire drilling states ("Free", "Point locked", "Axis locked", "Fully locked", "Shift wire" and "Align wire"). Each FSM transition is linked to an exactly defined condition, which is triggered by the user of the training system. A schematic diagram of the FSM states with its transitions can be found in Fig. 3.

Transition	Condition
#1	Collision detected between K-wire tip and bone
#2	K-wire tip immerged into the bone
#3	Drill button released and tool rotation stopped
#4	Pin driver leverage pressed
#5	Maximum possible K-wire length exceeded
#6	Reconnection of the K-wire to drill chuck started
#7	Target position of the K-wire alignment achieved
#8	Pin driver leverage released
#9	Drill button pressed and tool rotation started
#10	Retraction of the tool tip
#11	K-wire tip pullout over initial collision point
#12	Exceeded K-wire incidence angle

- "Point locked": After collision between drill tip and bone the drill tip position is locked. While the drill tip is touching the bone surface, the user can rotate the K-wire around the contact point. But if the incident angle is greater than 45° the "Free" mode becomes active and the K-wire slips over the bone surface. The transition to "Free" mode is also triggered, if the user pulls back the K-wire from the contact point between K-wire tip and bone.
- "Axis locked": If the K-wire has immerged several millimeters into the bone, the main axis of the K-wire rotation is locked. The K-wire can only move in axial forward or backward direction and rotate around its own axis. All other motions are blocked.
- "Fully locked": If the "Axis locked" mode of the FSM is active and the drill rotation is then interrupted, the transition to "Fully locked" is triggered. Because the K-wire is located inside the bone, its position as well as all rotations are completely blocked. Remaining bone meal within the bore-hole makes any movement impossible.
- "Shift wire": While a button for the pin driver leverage upon the haptic device tool head remains pushed, the K-wire is decoupled from the tool and the drill chuck position can be adjusted along the K-wire only along the axial backward and forward direction, until the maximum ranges are reached. By pulling back the drill chuck over the top maximum of the K-wire length, the current drill could be discarded. The K-wire remains stuck in the bone and the driller again can be freely moved through the 3D world ("Free"). Then it is possible to select a new K-wire via the GUI.
- "Align wire": In "Free" state, the user may realign an already discarded K-wire instead of choosing a new one. The haptic device automatically guides back the drill chuck to the top position of the discarded wire after manually triggering the FSM transition via the GUI.

Table 1 shows all trigger conditions for transitions between drill states.

To simulate each individual phase of the FSM with its haptic force-feedback easily we use a virtual fixtures approach.

2.3. Virtual fixtures based haptic feedback

So-called *virtual fixtures* are defined as abstract sensory information overlaid on top of reflected sensory feedback from a remote environment. The concept of virtual fixtures was first suggested by *Rosenberg* in 1993, as a guidance method for operators to do robotic remote control tasks [30]. These guidances are virtual surfaces lying as sensory information over a real workspace. The operator can perceive the overlay information by haptic or visual feedback. Virtual fixtures only interact with the user and not with the workspace, have no mass,

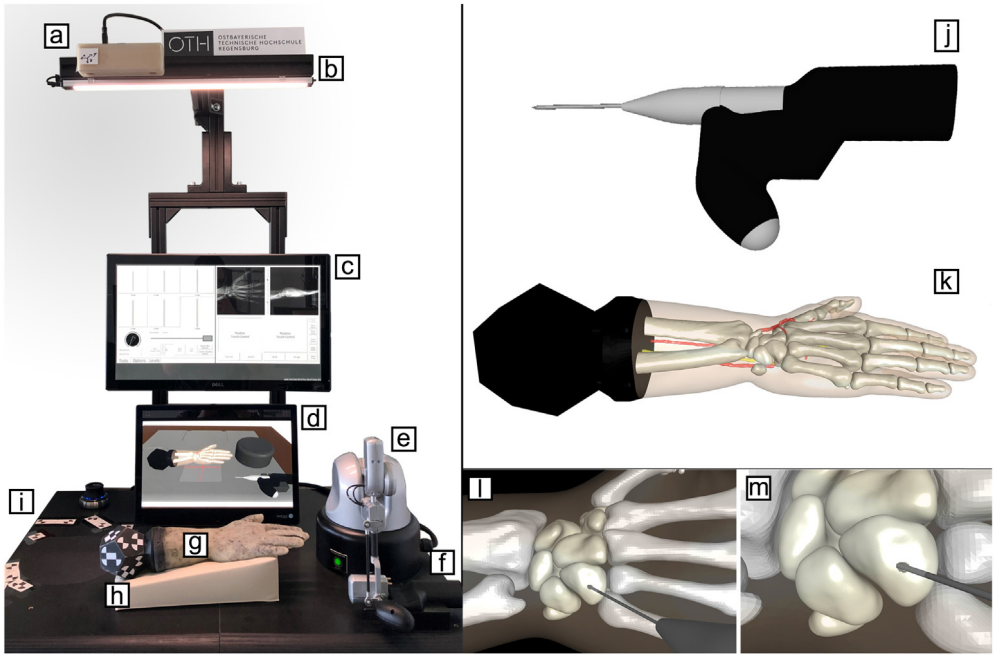

Fig. 2. Prototype setup of the VR-based HaptiVisT system for the training of K-wire drilling (left) with (a) real time tracking camera, (b) light source, (c) touchscreen monitor, (d) autostereoscopic 3D display with eye-tracking bar, (e) haptic force-feedback device, (f) 3D printed drilling hand piece, (g) hand phantom, (h) hand marker and (i) reference marker. On the top right the visualization of driller (j) and hand (k) can be seen, and consists of a mixture of surface and volume rendering. (l) and (m) depicts the virtual penetration of the K-wire into a hand bone. The rendering of (j)–(m) is displayed to the user via the 3D monitor (d).

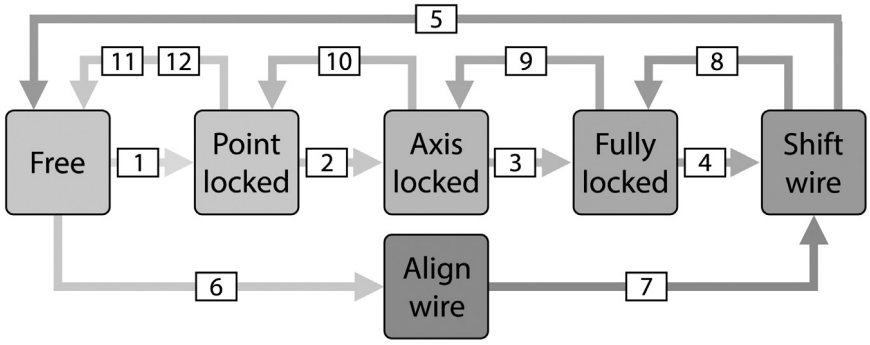

Fig. 3. Finite state machine (FSM) representing the decomposed K-wire behavior. The complex drilling task is separated into six discrete logical states (“Free”, “Point locked”, “Axis locked”, “Fully locked”, “Shift wire”, and “Align wire”) for an easy simulation and force-feedback control. A typical drilling process starts in “Free” mode. Any other state can only be reached by well-defined FSM state transitions triggered by the user. After a contact between bone and K-wire the FSM triggers the state transition #1 from “Free” to “Point locked” and the K-wire position is locked at the contact point. If the user drills the K-wire tip completely into the bone, the FSM enters via #2 the “Axis locked” state and all rotations except the rotation around the K-wire axis are also locked. By releasing the drill button (#3) the drilling is interrupted and all motion in translation and rotation are locked (“Fully locked”). If the pin driver leverage button is pressed, the K-wire length can be adjusted by a repeated use of transitions #4 and #8. Additionally, the K-wire can be completely discarded by a displacement of the drill handle over the K-wire maximum (#5). Back in the “Free” state an automated realignment of the K-wire can be initiated manually via the GUI (#6). If the “Align wire” state has reached its destination (#7), the drill handle automatically slides over the “Shift wire” state into “Fully locked” (#8). The drilling can be resumed on pressing the drill button (#9). By pulling out the K-wire of the drilling hole, the user reaches via “Point locked” (#10) the “Free” state (#11). The FSM transition #12 is triggered, if the user chooses a large incidence angle between K-wire axis and bone surface. Thus, the K-wire slides over the bone surface. See Table 1 for a compact listing of all trigger conditions enforcing the state transitions #1 to #12 and Section 3 for a visual FSM video representation.

no physical or mechanical constraints, can easily be prototyped or modified and can greatly enhance the human precision and performance. This virtual fixtures approach was further extended by *Joly and Andriot* who described them as virtual mechanisms, able to constrain the motion of the operator along selected degrees of freedom [31]. These restrictions provide the possibility to split a complex task into elementary subtasks, to make it safer and easier. For example, drilling a bore hole is represented as a 3D displacement vector of the tool position in axial direction. Virtual fixtures are used frequently as a way to simulate assembly constraints with a force-feedback device in the context of manufacturing (see e.g. [32]).

To implement virtual fixtures in our simulation we use proportional and derivative (PD) controllers. A PD is a very fast and common control algorithm to improve the stability of a tele-operative system and is often used in haptic systems, because they require response position data without time delay [33]. The position deviation and the angular orientation error between a reference setpoint (proxy) and the control point (cp) of the haptic device are calculated, as well as their derivatives, and multiplied by the proportional (P) and derivative (D) gains in order to produce forces and torques, which push the device towards this desired setpoint. The resulting damping force and torque pushes back the haptic device as long as its position matches the desired position. Since the force factors act against the direction of movement, the user cannot abandon the reference position. From the haptic force-feedback point of view, the “Free” and “Fully locked” states are very simple to implement using virtual fixtures. The states “Point locked”

and "Align wire", as well as "Axis locked" and "Shift wire" raise specific issues. Each state will be addressed independently according to haptic force and torque feedback in the following sections.

2.3.1. Free state

In "Free" mode, the driller can be moved freely. Consequently, the force tensors are zero and expressed as

$$\begin{aligned} F &= 0 \\ T &= 0, \end{aligned} \tag{1}$$

where

- F is the force vector calculated at the control point,
- T is the torque vector calculated at the control point.

2.3.2. Point locked state

As soon as the sharp tip of the K-wire touches the bone, it sticks to the contact point, that slipping becomes (almost) impossible. Actually, the haptic feeling is very similar in being attached to this contact point. Therefore, the "Point locked" state can be implemented as a translation-only PD controller, computed at the point of contact. Since the contact point at the K-wire tip and the control point location at the tip of the haptic device differ with an offset of up to 15 cm, the force components at the K-wire tip have to be transferred towards this control point. Thus, the haptic feedback is computed via

$$\begin{aligned} F &= F_{\text{tip}} \\ T &= \Delta_{\text{tip}} \times F_{\text{tip}}, \end{aligned} \tag{2}$$

where

- F_{tip} is the force vector at the K-wire tip,
- Δ_{tip} is the offset vector of the K-wire tip with respect to the control point.

The force vector F_{tip} is given by

$$F_{\text{tip}} = \mathbf{K}(X_{\text{lock}} - X_{\text{tip}}) - \mathbf{B}V_{\text{tip}}, \tag{3}$$

where

- $\mathbf{K}$ is the stiffness matrix and $\mathbf{B}$ the damping matrix at the K-wire tip,
- X_{lock} is the Cartesian position vector of the contact point, representing the proxy position of the haptic device,
- X_{tip} is the Cartesian position vector of the K-wire tip,
- V_{tip} is the Cartesian speed vector at the K-wire tip.

Since the contact point does not move, the derivative component has a damping effect. The matrices $\mathbf{K}$ and $\mathbf{B}$ can be build as follows:

$$\mathbf{K} = \begin{pmatrix} K_{\text{tip}} & 0 & 0 \\ 0 & K_{\text{tip}} & 0 \\ 0 & 0 & K_{\text{T}}^{\max} \end{pmatrix} \qquad \mathbf{B} = \begin{pmatrix} B_{\text{tip}} & 0 & 0 \\ 0 & B_{\text{tip}} & 0 \\ 0 & 0 & B_{\text{T}}^{\max} \end{pmatrix}, \tag{4}$$

using a normalized stiffness scalar at the tip of the K-wire

$$K_{\text{tip}} = \frac{K_{\text{T}}^{\max}}{1 + L^2 K_{\text{T}}^{\max}/K_{\text{R}}^{\max}}, \tag{5}$$

where

- B_{tip} is the damping scalar at the tip of the K-wire,
- $K_{\text{T}}^{\max}$ is the maximum acceptable stiffness scalar in translation at the device control point,
- $K_{\text{R}}^{\max}$ is the maximum acceptable stiffness scalar in rotation at the device control point,
- $L = \left\| \Delta_{\text{tip}} \right\|_2$ is the current length of the K-wire.

Normalization of K_{tip} is necessary, because it prevents instability of the system which results from the K-wire length. This offset between K-wire tip and control point requires a translation of both, force and rotation. However, a K-wire length of 6 cm only results already in a stiffness reduction by a factor 2 and consequently in a very soft contact between K-wire tip and bone. For this reason, the K-wire is aligned with axis Z of the control point, so that the Z components of $\mathbf{K}$ and $\mathbf{B}$ are the maximum stiffness values $K_{\text{T}}^{\max}$ and $B_{\text{T}}^{\max}$ respectively. As a result, we obtain a "Point locked" mode where the stiffness along the direction of the K-wire equals the maximum achievable by the haptic device, while being unconditionally stable.

During the drilling procedure, the progression into the bone is slow compared to the natural movement of the user. Therefore, it is sufficient to simulate the progression into the bone as a slow drift of the proxy position X_{lock} (see Eq (3)). As soon as the penetration depth is superior to the length of the cutting tip, rotations perpendicular to the K-wire axis become impossible, and the transition to the state "Axis locked" is triggered.

2.3.3. Axis locked state

The K-wire is a very stiff metal bar and the progression inside the bone during drilling is slow. Thus, the haptic feeling is similar to a hinge constraint, i.e. only one free rotation along the axis of the K-wire is possible. In order to achieve the maximum stiffness and damping scalars, force and torque are calculated in the control point with

$$\begin{aligned} F &= \mathbf{K}_{\text{IIR}}(X_{\text{proxy}} - X_{\text{cp}}) - \mathbf{B}_{\text{IIR}}V_{\text{cp}} \\ T &= \mathbf{K}_{\text{IIR}}(A_{\text{proxy}} \times A_{\text{cp}}) - \mathbf{B}_{\text{IIR}}V_{\text{cp}}, \end{aligned} \tag{6}$$

where

- X_{proxy} is the Cartesian position vector of the proxy position,
- X_{cp} is the Cartesian position vector of the control point position,
- A_{proxy} is the Cartesian orientation vector of the proxy,
- A_{cp} is the Cartesian orientation vector of the control point,
- V_{cp} is the Cartesian speed vector at the control point.

According to Eq (4), matrices $\mathbf{K}_{\text{IIR}}$ and $\mathbf{B}_{\text{IIR}}$ are still calculated in the definition of $\mathbf{K}$ and $\mathbf{B}$, but the stiffness K_{tip} and the damping B_{tip} on axes X and Y have been replaced by K_{n} and B_{n}:

$$\begin{aligned} K_{\text{n}} &= \alpha K_{\text{n-1}} + (1-\alpha)K_{\text{T}}^{\max} \\ B_{\text{n}} &= \alpha B_{\text{n-1}} + (1-\alpha)B_{\text{T}}^{\max}, \end{aligned} \tag{7}$$

where

- K_{n} is the stiffness scalar at time n,
- B_{n} is the damping scalar at time n,
- α is a constant control variable of value 0.999.

This results in time-discrete low-pass filtered stiffness and damping matrices

$$\mathbf{K}_{\text{IIR}} = \begin{pmatrix} K_{\text{n}} & 0 & 0 \\ 0 & K_{\text{n}} & 0 \\ 0 & 0 & K_{\text{T}}^{\max} \end{pmatrix} \qquad \mathbf{B}_{\text{IIR}} = \begin{pmatrix} B_{\text{n}} & 0 & 0 \\ 0 & B_{\text{n}} & 0 \\ 0 & 0 & B_{\text{T}}^{\max} \end{pmatrix}, \tag{8}$$

known as "Infinite Impulse Response" (IIR), which give a cut-off frequency of about 0.16 Hz with a sample rate of 1 kHz [34]. IIR allows a smooth transition over more than two seconds and avoids jerking in the haptic feedback. This prevents the user experience of a jerk in force entering the "Axis locked" state from the "Point locked" state.

2.3.4. Fully locked state

To calculate the force tensors of the "Fully locked" state, a simple PD is used to maintain the current position and orientation. The behavior is very similar to the "Axis locked" state, however all rotations are locked. The definition of the force and torque tensor is

$$\begin{aligned} F &= \mathbf{K}_{\text{IIR}}(X_{\text{proxy}} - X_{\text{cp}}) - \mathbf{B}_{\text{IIR}}V_{\text{cp}} \\ T &= \mathbf{K}_{\text{IIR}}(Q_{\text{proxy}} - Q_{\text{cp}}) - \mathbf{B}_{\text{IIR}}V_{\text{cp}}, \end{aligned} \tag{9}$$

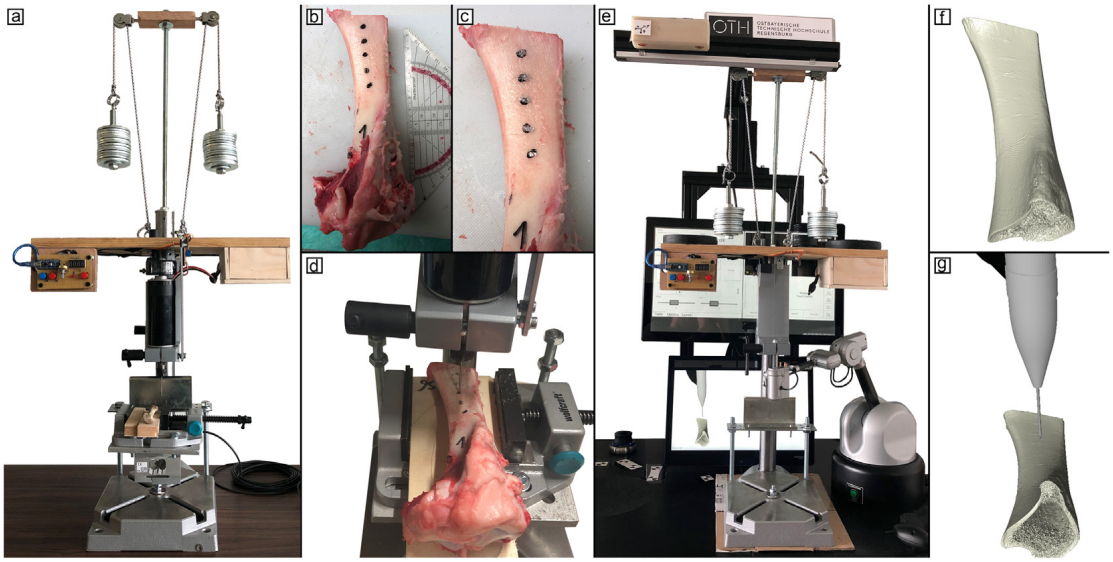

Fig. 4. (a) Experimental setup for drilling speed adjustment. A spindle motor with a K-wire drilling bit is clamped into a stationary drilling machine, which is mounted almost frictionless due to counterweights. A motor control unit regulates the supply voltage and thus the drilling speed of the motor. A load cell measures the axial thrust force, which is located between the workpiece clamping and the drilling machine stand. (b, c) Tibia pig bones are marked with a felt pen (b) and superposed barium-glue mixture (c) to ensure matching drilling points. (d) To prevent bones from moving during drilling, they are glued to a thin wooden plate, which is fixed in the clamping. (e) For the drilling model validation and parameter adjustment the haptic device is connected with the clamping to ensure identical drilling conditions. (f) Rendering of the virtual pig bone generated by segmentation of the micro CT. (g) Virtually pig bone drilling visualization.

where

- Q_{proxy} is the Cartesian rotation quaternion of the proxy orientation,
- Q_{cp} is the Cartesian rotation quaternion of the control point orientation.

2.3.5. Shift wire state

When pressing the pin driver leverage button, the user virtually disengages the K-wire from the driller head, but he can move the drilling machine only along the K-wire axis. The haptic feeling is very similar to a sliding hinge constraint, i.e. only one free rotation and one free translation along the axis of the K-wire is necessary. In order to calculate the sliding hinge constraint, any point along the axis of the K-wire can be chosen. In this work, the control point of the haptic device is used. As a result, the maximum acceptable stiffness and damping are achieved without any adjustment. Entering the state from "Fully locked" with homogeneous stiffness and damping, the same parameters can be kept. Compared to Eq (6) for calculating the "Axis locked" state tensors, only the sliding proxy position changes:

$$\begin{aligned} F &= \mathbf{K}_{\text{IIR}}(X_{\text{sp}} - X_{\text{cp}}) - \mathbf{B}_{\text{IIR}} V_{\text{cp}} \\ T &= \mathbf{K}_{\text{IIR}}(A_{\text{sp}} \times A_{\text{cp}}) - \mathbf{B}_{\text{IIR}} V_{\text{cp}}, \end{aligned} \tag{10}$$

where

- X_{sp} is the sliding Cartesian position vector of the proxy position,
- A_{sp} is the sliding Cartesian orientation vector of the proxy.

2.3.6. Align wire state

In practice, the "Align wire" state should be very similar to the "Point locked" state. The user can move the tool near to the K-wire rear tip, until it is axis-aligned and the drill chuck can penetrate the tool. However, because we are working in VR and there will be some inaccuracies in the system calibration and in the stereoscopic display, it might be very difficult for the user to find the rear tip of the K-wire exactly in the 3D space. Therefore, we propose a force guided alignment instead. When entering the state, a geodesic segment starting from the current pose of the tool and ending with the pose of the K-wire tip is generated. To avoid the risk of triggering transition #5 immediately, a small offset is added when entering the state "Shift wire" again. In the end, the behavior is actually identical to "Fully locked", but with a proxy that moves toward the rear tip of the K-wire. Therefore, the computation of F and T in Eq (9) changes to

$$\begin{aligned} F &= \mathbf{K}_{\text{IIR}}(X_{\text{rp}} - X_{\text{cp}}) - \mathbf{B}_{\text{IIR}} V_{\text{cp}} \\ T &= \mathbf{K}_{\text{IIR}}(Q_{\text{rp}} - Q_{\text{cp}}) - \mathbf{B}_{\text{IIR}} V_{\text{cp}}, \end{aligned} \tag{11}$$

where

- X_{rp} is the Cartesian proxy position vector moving to the rear tip position of the K-Wire,
- Q_{rp} is the Cartesian rotation quaternion moving to the rear tip orientation of the K-Wire.

2.4. Expert study design

The HaptiVisT training system for K-wire drilling with our new virtual fixtures approach was presented during the international FESSH conference 2018 in Copenhagen (Federation of European Societies for Surgery of the Hand). In a subjective formative evaluation experts were asked for their opinion about the force-feedback and the drilling behavior. After collecting sociodemographic data, a short system familiarization phase was followed by an open designed expert interview. For better interpretability the interviews were recorded on tape and transcribed using the MAXQDA software [35]. The sociodemographic data were evaluated based on the SPSS 25 software to get descriptive statistics and frequency analyses [36].

2.5. Experimental drilling speed adjustment

For a realistic K-wire drilling simulation the drilling speed parameters through bone must be adapted. For this purpose, we use an experimental setup, which can be seen in Fig. 4a. Inspired by several authors [37–41], the setup basically consists of a stationary drilling machine with a 12000 rpm spindle motor in the clamping. By varying the supply voltage, the motor can be set to fixed revolutions per minute, which is additionally monitored by a combination of a linear hall sensor and a small magnet attached to the spindle. Due to counterweights, the motor is attached almost frictionless to the greased guiding column. A

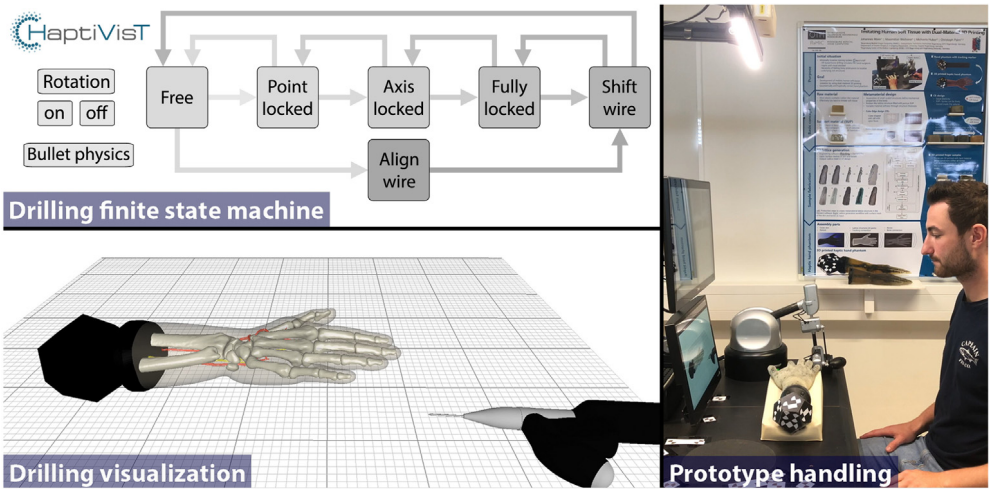

Fig. 5. Video frame of the virtual fixtures based force-feedback K-wire drilling simulation (find the full video in supplemental material). The video shows a parallel running video sequence of the drilling Finite State Machine (FSM, top left), the drilling visualization on the 3D monitor of the training system (lower left) and the real HaptiVisT prototype handling (right). While handling the force-feedback-assisted haptic device and hand phantom, the driller and hand rendering of the drilling visualization will follow the user's movement. Triggered by user interactions, the FSM changes drilling states via state transitions defined in Section 2.2, Fig. 3 and Table 1. The force-feedback transmitted to the user via the haptic device is controlled by the drilling FSM.

Table 2
Sociodemographic data of the expert surgeon evaluation at the international FESSH conference 2018. Each participant was asked about his/her age, sex, visual impairment, field of work, practical surgery experience in years, number of performed hand surgeries and training simulator experience. The evaluation distinguishes between more or less than 5 years of practical work experience and between more or less than 100 performed hand surgeries. N is the number of participants included in the statistic, numeric values are means, frequencies others. SD corresponds to the standard deviation of the mean value.

Case		Value	N
Age		42.28 (SD = 10.41)	26
Sex	male	17 (65.4%)	26
	female	9 (34.6%)	26
Impairment	visual	10 (38.5%)	26
	no	16 (61.5%)	26
Handedness	right	25 (96.2%)	26
	left	1 (3.8%)	26
Field of work	hand surgery	16 (61.5%)	25
	traumatology	6 (23.1%)	25
	other	3 (15.4%)	25
Practical surgery experience	≥ 5 years	21 (80.8%)	26
	< 5 years	5 (19.2%)	26
Performed hand surgeries	≥ 100	21 (80.8%)	26
	< 100	5 (19.2%)	26
Training simulator experience	yes	1 (3.8%)	26
	no	25 (96.2%)	26

continuous thrust force can be applied by placing weights onto the drill rest. A load cell between the drilling machine stand and a clamping for workpieces measures axial drilling forces up to 100N. Thus, axial guided K-wire drillings with constant thrust force and rotation speed could be performed. The forces at the load cell are amplified and then recorded via the HBM CATman AP V5.0.1 software in a 300 Hz rhythm [42].

To determine the relationship between drilling thrust force, rotational speed and feed rate, we used four equally shaped tibia pig bones from a local butcher's shop. Pig bones represent a good likeness with human bone in regard to their close conformity of bone density [43]. Drilling on pig bones was performed in the real world on the experimental setup and in virtual reality on the HaptiVisT training system to adjust the drilling parameters. For virtual drilling a micro CT scan of each pig bone was generated. To ensure that drilling is comparable, each pig bone is freed from muscle and fatty tissue in order to mark five drilling points on the inner tibia at 1 cm intervals with a felt pen (Fig. 4b) and by a superposed barium-glue mixture (Fig. 4c). The barium serves later as marker in the CT scans.

After gluing the pig bones onto wooden plates, drilling on the experimental setup was performed at all five marked drill points and 3 mm vertically right and left for data averaging (Fig. 4d). The constantly applied thrust force was measured by the load cell at different rotation speeds, starting at 900, 1200, 1500 up to 1800 rpm. After manually approaching a drilling point with the K-wire tip, time measurement started simultaneously with the motor rotation to determine the drilling time through cortical bone. Calculation of the drilling feed rate in millimeter per second results from the corticalis thickness, measured on the segmented bone from the CT scan, and the drilling time through this cortical bone.

According to the empirical force model of *Chi et al. (2005)* the bone density ρ_{bone} in [g/cc] could be determined by

$$\rho_{\text{bone}} = \left(\frac{F_{\text{Th}}}{C_T} N^{-C_N} f^{-C_f} \right)^{1/C_\rho}, \tag{12}$$

with the thrust force F_{Th}, the spindle speed N of the drill bit in rotations per minute and the feed rate f in [mm/s]. $C_T = 134.6097$, $C_N = -0.3327$, $C_f = 0.5189$ and $C_\rho = 1.1841$ are validated constants [39]. Thus after determining the mean bone density using all spindle speeds and measured feed rates of the experimentally drilled holes, feed rates of variable applied thrust forces can be calculated in the drilling simulation using (12) resolved to f.

3. Results

The behavior of K-wire drilling could be easily divided into few drilling subtasks and combined in a FSM with well-defined transitions. The virtual fixtures based haptic force-feedback calculation operates stable with a constant thread rate of 1000 Hz. A video summary of the resulting drilling simulation including the animated FSM, the drilling simulation and the prototype handling with force-feedback can be found in Fig. 5.

26 expert surgeons were asked to evaluate the force-feedback assisted drilling at the FESSH conference in Copenhagen 2018. The sociodemographic data can be found in Table 2. 17 subjects (65.4%) were male and nine (34.6%) female. The average age of participants was 42.28 years (SD = 10.41), with the youngest participant being 30 and the oldest being 67 years old. Participants had an average of 14.20 years of practical surgical experience, with 80.8% having

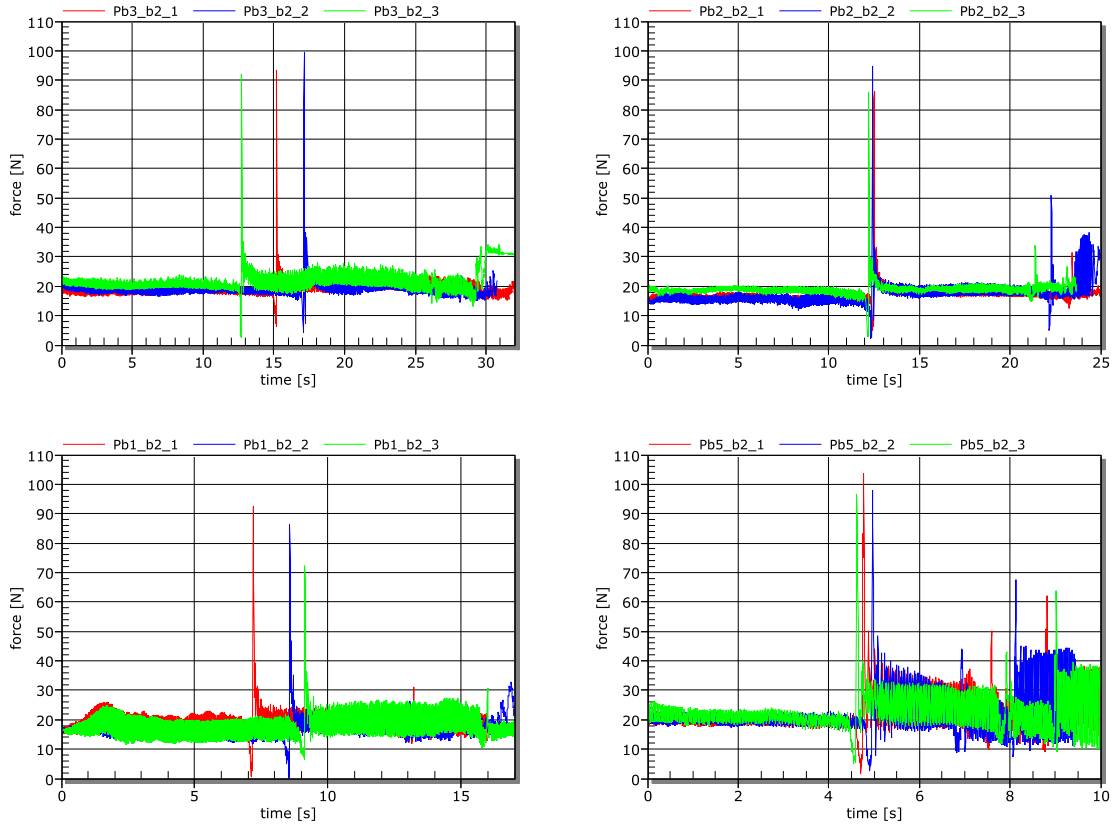

Fig. 6. Force–time graphs of experimental pig bone K-wire drilling. To determine the drilling duration through the first cortex, K-wires are drilled standardized into four pig bones. The axial force measurement by a load cell starts simultaneously with the drill rotation. Big force peaks represent the slip of the drill into the spongiosa after drilling the first cortex. The time point of the force peak determines the duration between start of drilling and penetration of the cortex. Each plot represents three drilling procedures through the same pig bone (e.g. the first pig bone Pb1) and a marked drilling point (here the second bone marker b2) to calculate a median value. The first drilling is made exactly through this marked drilling point (e.g. Pb1_b2_1 indicates the bone marker two (b2) of pig bone one (Pb1) is drilled exactly through the marker (1), red graph) and 3 mm left (e.g. Pb1_b2_2, blue graph) or 3 mm right (e.g. Pb1_b2_3, green graph). For each bone we used an another drilling speed, measuring the difference in duration. The drill rotation speed rises from 900 (upper left, Pb3) over 1200 (upper right, Pb2) and 1500 (lower left, Pb1) to 1800 rpm (lower right, Pb5) by using always the same constant thrust force. As can be seen, the duration to cross the cortex increases using smaller rotational speed.

Table 3
To calculate the feed rate of K-wire drilling through bone, we need the drilling duration and the cortical bone thickness. The table shows the experimentally determined median values for the cortical thickness x [mm] and the drilling time t [s] through corticalis. x is measured manually using the micro CT scans, t is taken from the first force peak of the force–time graphs (see Fig. 6) and the **median feed rate f** [mm/s] as well as their variance is calculated from x and t. Median x and t values are taken from four pig bones (Pb5, Pb1, Pb2, Pb3) with different rotation speeds (1800, 1500, 1200 and 900 rpm) and at five different drill points (b1, b2, b3, b4, b5). To calculate these median values drilling is performed at the marked drill points as well as 3 mm left and 3 mm right next to the marker.

	b1			b2			b3			b4			b5		
	x	t	**f**	x	t	**f**	x	t	**f**	x	t	**f**	x	t	**f**
$Pb5_{1800}$	2.34	4.38	**0.54**	2.41	4.77	**0.50**	2.70	6.47	**0.45**	2.96	6.89	**0.43**	3.70	9.75	**0.35**
variance	0.03	0.07	**0.00**	0.00	0.03	**0.00**	0.08	0.10	**0.00**	0.03	0.16	**0.00**	1.06	6.05	**0.06**
$Pb1_{1500}$	2.92	7.87	**0.37**	3.00	8.56	**0.36**	3.22	8.25	**0.38**	4.50	9.56	**0.45**	4.43	11.40	**0.39**
variance	0.02	1.02	**0.00**	0.02	0.99	**0.00**	0.01	0.10	**0.00**	0.13	0.73	**0.00**	0.08	52.84	**0.02**
$Pb2_{1200}$	2.63	11.35	**0.23**	2.64	12.40	**0.22**	3.09	16.09	**0.19**	3.50	17.48	**0.20**	4.83	24.46	**0.24**
variance	0.01	2.33	**0.00**	0.11	0.02	**0.00**	0.03	5.60	**0.00**	0.14	3.52	**0.00**	0.78	86.34	**0.01**
$Pb3_{900}$	2.37	14.50	**0.16**	2.54	15.19	**0.17**	2.71	18.13	**0.15**	3.97	31.19	**0.10**	3.90	35.99	**0.11**
variance	0.01	1.48	**0.00**	0.01	4.85	**0.00**	0.01	1.62	**0.00**	0.51	60.69	**0.00**	1.64	52.73	**0.00**

performed more than 100 minimally invasive hand surgeries and 19.2% less than 100. Hence, the majority of participants had sufficient expert status. 61.5% of the participants have practiced hand surgery, 23.1% were experts in traumatology and 15.4% came from other areas (plastic or nerve surgery). 38.5% of the participants suffered from visual impairment, 96.2% were right-handed and had no experience with computer training simulators. Force-feedback, haptic device stiffness and tool vibration were rated positively and without any further need for optimization.

All subjects sensed the haptic force-feedback as very good and authentic with great resistance. The behavior was classified as accurate and especially the "Point locked" mode was evaluated as very realistic. As only drawback mentioned, the drilling speed behavior had to be adjusted, because compared to reality, the proportions between cancellous and cortical bone seems to be not yet accurate. Thus, the cortical bone was predominantly described as too hard and the needed cortical drilling time as too long.

The duration for drilling the cortical bone can be determined from the experimentally obtained force–time graphs. Due to the transition from cortical to the cancellous bone, the drill slides quickly to the counter corticalis, stops and produces a force peak. Four force–time graphs can be seen in Fig. 6. Each graph was obtained at a different pig

bone representing a different rotation speed at the same marked drill point. The feed rate is then calculated from the drilling time through cortex and the measured cortical thickness from the micro CT. Median values and variances of measured time, thickness and calculated feed rate can be found in Table 3. The drilling speed increases as expected with higher rotation speed. By using these median feed rate values and the corresponding thrust force, averaged up to the first force peak, in Eq (12), we can determine a median bone density of 2.4195 g/cc as function of rotational speed and thrust force. With Eq (12) resolved to f we can now calculate any feed rate value for different rotation speeds and thrust forces. Since the simulation thread for feed rate calculation and K-wire motion is clocked to a frequency of 1000 Hz, a constant motion of the haptic device proxy position X_{tip} in Eq (3) is guaranteed. Within the virtual environment, the thrust force can be directly received from the haptic device and the rotational speed via a stepless regulatable button at the drilling device. To verify the model, the experimental setup was modified, so that the end of the haptic device could be clamped in the drilling unit (Fig. 4e). Several drill points have been drilled virtually using constant rotation speeds and thrust forces which successfully validated a matching of virtual and real drilling (Fig. 4f and g).

4. Discussion

The proposed method for VR-based drilling simulation combines the approaches of *Tsai et al. (2007)* [4] and *Vankipuram et al. (2010)* [12]. A complete drilling simulation system was created covering the entire drilling process. But this drilling process is divided into individual sub-processes using virtual fixtures. This makes it easy to treat, simulate and calculate the haptic force-feedback completely separately. The haptic force-feedback was rated as authentic and good, but improvements in drilling speed were necessary. Thus, the subjective formative evaluation was followed by an objective experimental setup to measure actual force–time graphs during real bone drilling and determine the realistic feed rate through cortical bone. The validation of the drilling model with the same experimental setup but drilling virtually makes the system even more realistic. Since our haptic device can only apply a continuous force in translation of 3N and a maximum of 10N [17], the thrust force applied by the user of the training system is adjusted with a factor two. To transfer the drilling without restrictions the desktop version of the haptic device must be exchanged for a stronger version. For this purpose, the drilling simulation has already been successfully tested in combination with the stronger non-desktop version "Virtuose 6D" from Haption© with a continuous force in translation of 9.5N and a maximum of 35N.

5. Conclusion

In this work, we have presented a new virtual fixture based force-feedback calculation approach for the simulation of bone drilling behavior in the context of a VR hand surgery training system. Our work was evaluated by a total of 26 experienced surgeons who adjudged the drilling and the resulting force-feedback as "very realistic" and "accurate". The subjective formative evaluation was followed by an objective force measuring setup to determine the realistic feed rate through cortical bone.

Currently, the HaptiVisT system is limited to the training of K-wire drilling through hand bones. In future work, the principle of linear drilling with virtual fixtures can be transferred to any other surgical field related to bone drilling (e.g. knee or hip surgery). The variety of tools must be expanded, including twist drills and screws, to stabilize severe bone fractures with plate osteosynthesis.

Declaration of competing interest

The authors declare that they have no known competing financial interests or personal relationships that could have appeared to influence the work reported in this paper.

Acknowledgments

We acknowledge the support from the Deutsche Forschungsgemeinschaft (DFG) in frame of the program "Forschungsgeräte" (INST 102/11 – 1 FUGG) for using the micro CT.

This work was funded by the German Federal Ministry of Education and Research with grant 16SV7559, grant 16SV7560 and grant 16SV7562 and supported by the Bavarian Academic Forum (BayWISS) - Doctoral Consortium "Health Research", funded by the Bavarian State Ministry of Sciences, Research and the Arts.

Ethical approval

For this type of study formal consent is not required.

Informed consent

This article does not contain patient data.

Appendix A. Supplementary data

Supplementary material related to this article can be found online at https://doi.org/10.1016/j.compbiomed.2019.103473.

References

[1] B.B. Franssen, A.H. Schuurman, A.M. Van der Molen, M. Kon, One century of kirschner wires and kirschner wire insertion techniques: A historical review, Acta Orthopaed. Belg. 76 (1) (2010) 43–53.
[2] D.A. Gould, N. Chalmers, S.J. Johnson, C. Kilkenny, M.D. White, B. Bech, L. Lonn, F. Bello, Simulation: Moving from technology challenge to human factors success, Cardiovasc. Inter. Rad. 35 (3) (2012) 445–453.
[3] J. Maier, M. Huber, U. Katzky, J. Perret, T. Wittenberg, C. Palm, Force-feedback-assisted bone drilling simulation based on CT data, in: Bildverarbeitung für die Medizin 2018, Springer, Berlin, Heidelberg, 2018, pp. 291–296.
[4] M.-D. Tsai, M.-S. Hsieh, C.-H. Tsai, Bone drilling haptic interaction for orthopedic surgical simulator, Comput. Biol. Med. 37 (12) (2007) 1709–1718.
[5] I. Badash, K. Burtt, C.A. Solorzano, J.N. Carey, Innovations in surgery simulation: a review of past, current and future techniques, Ann. Transl. Med. 4 (23) (2016) 453.
[6] R. McCloy, R. Stone, Virtual reality in surgery, BMJ 323 (7318) (2001) 912–915.
[7] J. Wu, G. Yu, D. Wang, Y. Zhang, C.C.L. Wang, Voxel-based interactive haptic simulation of dental drilling, in: 29th Computers and Information in Engineering Conference, Parts A and B, vol. 2, 2009, pp. 39–48.
[8] J.L. Griffith, P. Voloschin, G.D. Gibb, J.R. Bailey, Differences in eye-hand motor coordination of video-game users and non-users, Percept. Motor Skill 57 (1) (1983) 155–158.
[9] J.C. Rosser, P.J. Lynch, L. Cuddihy, D.A. Gentile, J. Klonsky, R. Merrell, The impact of video games on training surgeons in the 21st century, Arch. Surg. 142 (2) (2007) 181–186.
[10] N.E. Seymour, A.G. Gallagher, S.A. Roman, M.K. O'Brien, V.K. Bansal, D.K. Andersen, R.M. Satava, Virtual reality training improves operating room performance: Results of a randomized, double-blinded study, Ann. Surg. 236 (4) (2002) 458–464.
[11] J. Maier, M. Weiherer, M. Huber, C. Palm, Imitating human soft tissue on basis of a dual-material 3D print using a support-filled metamaterial to provide bimanual haptic for a hand surgery training system, Quant. Imaging Med. Surg. 9 (1) (2018) 30–42.
[12] M. Vankipuram, K. Kahol, A. McLaren, S. Panchanathan, A virtual reality simulator for orthopedic basic skills: A design and validation study, J. Biomed. Inform. 43 (5) (2010) 661–668.
[13] G. Lopez, R. Wright, D. Martin, J. Jung, D. Bracey, R. Gupta, A cost-effective junior resident training and assessment simulator for orthopaedic surgical skills via fundamentals of orthopaedic surgery: Aaos exhibit selection, J. Bone Joint Surg. 97 (8) (2015) 659–666.
[14] T. Seah, A. Barrow, A. Baskaradas, C. Gupte, F. Bello, A virtual reality system to train image guided placement of kirschner-wires for distal radius fractures, in: Biomedical Simulation. 6th International Symposium, ISBMS 2014, in: Lecture Notes in Computer Science, vol. 8789, Springer, Cham, 2014, pp. 20–29.
[15] F. Wu, X. Chen, Y. Lin, C. Wang, X. Wang, G. Shen, J. Qin, P.-A. Heng, A virtual training system for maxillofacial surgery using advanced haptic feedback and immersive workbench, Int. J. Med. Robot. 10 (1) (2014) 78–87.
[16] Y. Lin, X. Wang, F. Wu, X. Chen, C. Wang, G. Shen, Development and validation of a surgical training simulator with haptic feedback for learning bone-sawing skill, J. Biomed. Inform. 48 (2014) 122–129.

[17] J. Perret, Haption, 2019, https://www.haption.de, (Accessed 23 July 2019).
[18] Arthrex Inc., Arthrex drill saw mini 300 system, 2019, https://www.arthrex.com/imaging-resection/300-power-system, (Accessed 23 July 2019).
[19] C.M. Grossmann, A new AS-display as part of the MIRO lightweight robot for surgical applications, Proc. SPIE 7524 (2010) 7524–7524 – 12.
[20] SeeFront GmbH, Seefront - 3D getting real, 2019, https://www.seefront.com, (Accessed 11 September 2019).
[21] F. Barbagli, S. Chan, F. Conti, S. Grange, D. Morris, D. Ruspini, C. Sewell, O. Khatib, K. Salisbury, N. Blevins, Chai3d, 2019, http://www.chai3d.org, (Accessed 23 July 2019).
[22] E. Coumans, R. Ponomarev, J. McCutchan, N. Presson, G.V. den Bergen, C. Ericson, P. Knight, O. Kniemeyer, S. Hobbs, P. Terdiman, D. Gregorius, E. Catto, F. Leon, E. Sunshine, S. Baker, J. Lee, V. Klementjev, M. Svanfeldt, M. Hennix, A. Shek, Bullet 2.83 physics SDK manual, 2015, https://github.com/bulletphysics/bullet3/blob/master/docs/Bullet_User_Manual.pdf, (Accessed 23 July 2019).
[23] J. Maier, S. Haug, M. Huber, U. Katzky, S. Neumann, J. Perret, M. Prinzen, U. Scorna, K. Weber, T. Wittenberg, R. Wöhl, C. Palm, Developement of a haptic and visual assisted training simulation concept for complex bone drilling in minimally invasive hand surgery, in: Proc of the 31th Int Congress and Exhibition of Comp Assisted Radiology and Surgery, CARS, 2017, pp. 135–136.
[24] M.E.H. Boeckstyns, M. Richter, Fractures of the Hand and Carpus: FESSH 2018 Instructional Course Book, Thieme, 2018.
[25] S. Karmani, F. Lam, The design and function of surgical drills and k-wires, Curr. Orthopaedics 18 (6) (2004) 484–490.
[26] P. Adamczyk, The anthology of the finite state machine design patterns, in: Proc of the 10th Conference on Pattern Languages of Programs PLoP, 2003.
[27] J.-F. Aubry, N. Brinzei, Systems Dependability Assessment: Modeling with Graphs and Finite State Automata, Wiley-ISTE, London, 2015.
[28] J. Sakarovitch, R. Thomas, Elements of Automata Theory, in: Encyclopedia of Mathematics and its Applications, Cambridge University Press, London, 2009.
[29] F. Wagner, R. Schmuki, T. Wagner, P. Wolstenholme, Modeling Software with Finite State Machines: A Practical Approach, Auerbach Publications, Boston, MA, USA, 2006.
[30] L.B. Rosenberg, Virtual fixtures: Perceptual tools for telerobotic manipulation, in: Proc of 1993 IEEE Virtual Reality Annual International Symposium, 1993, pp. 76–82.
[31] L.D. Joly, C. Andriot, Imposing motion constraints to a force reflecting telerobot through real-time simulation of a virtual mechanism, in: Proc of 1995 IEEE International Conference on Robotics and Automation, vol. 1, pp. 357–362.
[32] L. Tching, G. Dumont, J. Perret, Interactive simulation of CAD models assemblies using virtual constraint guidance, Int. J. Interact. Des. Manuf. 4 (2) (2010) 95–102.
[33] B. Liacu, I.C. Morărescu, S.I. Niculescu, C. Andriot, D. Dumur, P. Boucher, F. Colledani, Proportional-derivative (PD) controllers for haptics subject to distributed time-delays: Aetrical ap geomproach, in: 2012 12th International Conference on Control, Automation and Systems, 2012, pp. 1605–1610.
[34] J.G. Proakis, D.G. Manolakis, Digital Signal Processing (3rd Ed.): Principles, Algorithms, and Applications, Prentice-Hall International, Inc., USA, 1996.
[35] VERBI Software GmbH, MAXQDA - The art of data analysis, 2019, https://www.maxqda.de, (Accessed 23 July 2019).
[36] International Business Machines Corporation, IBM SPSS Statistics, 2019, http://www.ibm.com, (Accessed 23 July 2019).
[37] K. Alam, A.V. Mitrofanov, V.V. Silberschmidt, Experimental investigations of forces and torque in conventional and ultrasonically-assisted drilling of cortical bone, Med. Eng. Phys. 33 (2) (2011) 234–239.
[38] K.N. Bachus, M.T. Rondina, D.T. Hutchinson, The effects of drilling force on cortical temperatures and their duration: an in vitro study, Med. Eng. Phys. 22 (10) (2000) 685–691.
[39] X. Chi, Q. Niu, V.S. Thakkar, M.C. Leu, Development of a bone drilling simulation system with force feedback, in: Proceedings of IMECE2005 2005 ASME International Mechanical Engineering Congress and Exposition, 2005, pp. 83–89.
[40] J. Lee, B.A. Gozen, O.B. Ozdoganlar, Modeling and experimentation of bone drilling forces, J. Biomech. 45 (6) (2012) 1076–1083.
[41] W.A. Lughmani, K. Bouazza-Marouf, I. Ashcroft, Drilling in cortical bone: a finite element model and experimental investigations, J. Mech. Behav. Biomed. Mater. 42 (2015) 32–42.
[42] Hottinger Baldwin Messtechnik GmbH, HBM Catman easy - software for data acquisition, visualization, analysis and reporting of measurement data for your PC, 2019, https://www.hbm.com/de/2472/support-downloads-catman, (Accessed 23 July 2019).
[43] A.I. Pearce, R.G. Richards, S. Milz, E. Schneider, S.G. Pearce, Animal models for implant biomaterial research in bone: A review, Eur. Cell Mater. 13 (2007) 1–10.